Short Communication

Effect of Bath ZrO$_2$ Concentration on the Properties of Ni-Co/ZrO$_2$ Coatings Obtained by Electrodeposition

Sirui Li[1,2], Pengfei Ju[3], Yapeng Zhang[1], Xiaofeng Zhang[1], Xuhui Zhao[1,*], Yuming Tang[1*], Yu Zuo[1], Ling Pu[2]

[1] Beijing Key Laboratory of Electrochemical Process and Technology for Materials, Beijing University of Chemical Technology, Beijing, 100029, China
[2] Sichuan Province Academy of Industrial Environmental Monitoring, Chengdu, 610041, China
[3] Shanghai Aerospace Equipment Manufacture Co. Ltd., Shanghai, 200245, PR China
[*]E-mail: xhzhao@mail.buct.edu.cn

Ni-Co/ZrO$_2$ composite coatings with different ZrO$_2$ contents have been prepared by electrodeposition. The ZrO$_2$ content was controlled by deploying different ZrO$_2$ particle concentrations in the bath. Micrographs, composition, microstructure, micro-hardness, and wear resistance of the composite coatings have been studied. The results showed that the ZrO$_2$ content in the coatings increased as the ZrO$_2$ concentration in the bath was increased up to 15 g/L, whereupon the highest micro-hardness and best wear resistance were obtained. When the bath ZrO$_2$ concentration exceeded 15 g/L, the ZrO$_2$ content in the coatings decreased, leading to inferior properties.

1. INTRODUCTION

Metal matrix composite coatings prepared by electrodeposition have attracted much attention in recent years. During the electrodeposition process, the reinforcing particles, which are suspended in the electrolyte, are co-deposited with metallic ions and embedded in the growing metal matrix. Compared with metal or alloy coatings, composite coatings have many excellent properties, such as higher hardness, better wear and corrosion resistances, high-temperature corrosion resistance, and oxidation resistance [1–5]. Different types of particles, such as SiC, Al$_2$O$_3$, diamond, and WC, have been commonly used as reinforcing particles [6–8]. Besides, ZrO$_2$ has many good physical and chemical properties and has been widely used in industrial fields. Researchers have also prepared ZrO$_2$ composite coatings, such as Ni-W/ZrO$_2$ [9,10] and Ni/ZrO$_2$ [11], and found these materials to show

good properties in terms of hardness, adhesion ability, and wear resistance. Ni-Co coatings have been widely used as important engineering materials in industry because of their high strength, good corrosion resistance, and wear resistance [12–16]. Li et al. [14] prepared Ni-Co alloys by pulse electrodeposition and found that peak current density significantly affected their composition, microstructure, surface morphology, fine grain size, micro-hardness, and tensile strength. Compared with Ni-Co deposits produced by Direct current (DC) plating, the described Ni-Co alloys had substantially higher hardness. Srivastava et al. [15] prepared Ni-Co alloys with varying Co contents by employing a sulfamate electrolyte. They observed that the alloy co-deposition was of an anomalous type. Cross-section micro-hardness measurements indicated that the hardness increased with increasing Co content up to 50 wt.% and then decreased thereafter. However, polarization and Electrochemical impedance spectroscopy (EIS) studies indicated that Ni-20% Co alloy exhibited better corrosion resistance than other Ni-Co alloys. Zamani et al. [16] also studied the effect of Co content on the mechanical properties of electrodeposited Ni-Co alloy. They found that with increasing Co content up to 45% in the alloy coating, the grain size decreased and consequently the hardness and strength of the alloy increased. Further enhancement of the Co content up to 55% led to small decreases in hardness and strength. The maximum ductility was observed for an Ni−25%Co coating due to its relatively small grain size and compact structure.

In the present study, Ni-Co/ZrO_2 composite coatings have been prepared, and the effects of ZrO_2 concentration in the bath on the composition, microstructure, micro-hardness, and wear resistance have been investigated.

2. EXPERIMENTAL

The substrate material was Q235 carbon steel. It was cut into pieces of dimensions 200 mm × 100 mm × 2 mm so that the electrodeposition process could be easily carried out. The nominal composition (wt.%) of Q235 carbon steel is C 0.15%, Mn 0.40%, Si 0.20%, P 0.030%, and S 0.025%, with a balance of Fe.

Each Q235 carbon steel specimen was first pretreated according to the following procedure: (1) abrasion with silicon carbide papers from 200# to 1000#, (2) degreasing for about 5 min, (3) etching in HCl and H_2SO_4 solution for about 30 s. Each specimen was then rinsed with deionized water and electroplated with Ni-Co/ZrO_2 coatings in the following electrolyte: 300 g/L Ni$(NH_2SO_3)_2 \cdot 4H_2O$, 13.7 g/L Co$(NH_2SO_3)_2 \cdot 4H_2O$, 6 g/L $NiCl_2$, 30 g/L H_3BO_3, 0.2 g/L sodium dodecyl benzene sulfonate (SDBS), 5–20 g/L ZrO_2 (pH 4). The plating temperature was set at 45 °C and the applied current density was 1.5 A/dm^2 for 30 min. The coatings were prepared by both mechanical stirring and ultrasonication dispersion, and the thicknesses obtained were about 30 μm.

Scanning electron microscope (SEM, S-4700) was used to examine the surface morphologies and thicknesses of the deposited coatings, and Energy disperse spectroscopy (EDS) was used to determine their compositions. X-Ray Diffraction (XRD, D/max2500VB2+/PC) was used to analyze the crystal structures, and grain size was also calculated with this method.

The micro-hardness was measured at least ten times for each coating sample, using a micro-hardness tester (HM2000, Fischer, Germany). The average micro-hardness value of the coating was taken.

According to ASTM D4541-09 (Standard Test Method for Pull-Off Strength of Coatings), the adhesive strength of the film to the stainless steel substrate was measured using a Positest pull-off adhesion tester. The abrasive resistance was measured with a UMT-3 friction testing machine.

3. RESULTS AND DISCUSSION

3.1. Micrographs and compositions of the composite coatings

Figure 1 shows the surface morphologies of Ni-Co/ZrO_2 coatings obtained in baths containing different concentrations of ZrO_2. It can be seen that all of the coatings were compact and uniform, and that the white area was maximized when the ZrO_2 concentration was 15 g/L. This can be interpreted in terms of the coating having the highest ZrO_2 content under these conditions, as corroborated by EDS measurements (Table 1). Table 1 shows the variation of ZrO_2 content in the Ni-Co/ZrO_2 coating with its concentration in the bath. The ZrO_2 content increased from 1.51 to 4.08 wt.% as its concentration in the bath was increased from 5 to 15 g/L. However, when the bath ZrO_2 concentration was further increased, the ZrO_2 content in the coating decreased.
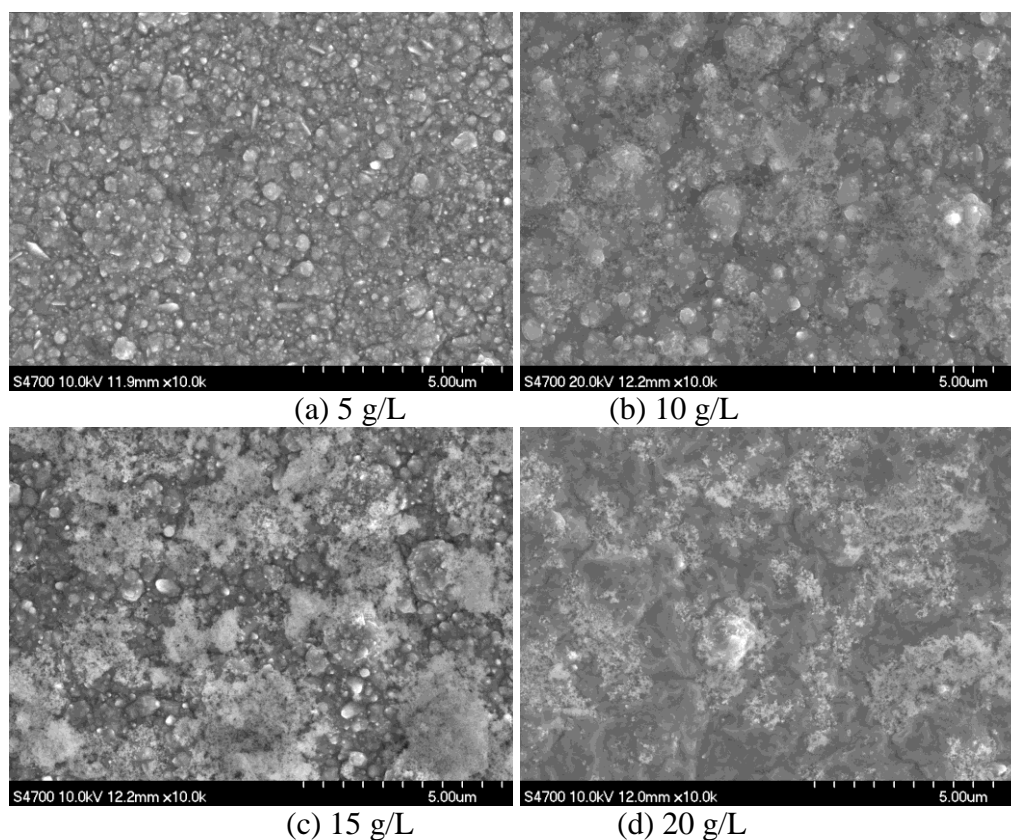

| (a) 5 g/L | (b) 10 g/L |
| (c) 15 g/L | (d) 20 g/L |

Figure 1. Surface morphologies of Ni-Co/ZrO_2 coatings obtained in baths containing different concentrations of ZrO_2 (plating temperature: 45 °C, current density: 1.5 A/dm^2, time: 30 min).

Table 1. ZrO$_2$ contents in Ni-Co/ZrO$_2$ coatings obtained in baths containing different concentrations of ZrO$_2$ (plating temperature: 45 °C, current density: 1.5 A/dm^2, time: 30 min).

ZrO$_2$ conten	5 g/L	10 g/L	15 g/L	20 g/L
Ni (wt%)	63.97	59.15	58.60	66.18
Co (wt%)	34.52	36.91	37.15	30.18
Zr (wt%)	1.51	3.94	4.08	3.64

The process of incorporating particles into a metal matrix involves five consecutive steps [1,17]: (1) formation of an adsorbed ionic cloud on the surface of the particles, (2) convection of the particles towards the cathode, (3) diffusion of the particles through the diffusion double layer, (4) adsorption of the particles surrounded by the ionic cloud on the cathode surface, (5) reduction on the cathode of a fraction of the ions adsorbed on the surface of the particles and incorporation of particles into the growing deposit. In our study, increasing the concentration of ZrO$_2$ particles in the bath led to an increase in the amount of adsorbed ZrO$_2$ nanoparticles on the growing deposit surface, resulting in more nanoparticles becoming incorporated into the coating. However, when the ZrO$_2$ concentration in the bath was increased to 20 g/L, a decrease in the ZrO$_2$ particle content in the coating was observed. Laszczyńska et al. [17] observed that the ZrO$_2$ content in a coating increased to a maximum of 4.5 wt.% when the ZrO$_2$ concentration in the bath was increased to 20 g/L. When the ZrO$_2$ concentration was further increased to 25 g/L, the ZrO$_2$ content decreased. Gül et al. [18] also found that when the bath SiC concentration was increased to 20 g/L, the SiC content reached a maximum value and decreased when the bath SiC concentration was further increased. They attributed this decrease to a shielding effect and agglomeration of the nanoparticles in the bath at high particle concentration [18].

3.2. Microstructure of the composite coatings

Figure 2 shows the XRD patterns of Ni-Co/ZrO$_2$ coatings prepared in baths containing different ZrO$_2$ concentrations. Researchers have found that Ni-Co coatings retain the *fcc* structure of Ni. An Ni-Co coating exhibits preferential (200) crystallographic orientation. However, the intensity of the (111) texture increases substantially at the expense of that of the (200) texture upon the incorporation of ZrO$_2$. It has been shown that the texture of electrodeposits depends on the surface energy of the growing crystallographic planes [19]. However, the consolidation of (111) texture can be attributed to the effect of ZrO$_2$ particles on the surface energy of growing crystallographic planes.

Table 2 shows the grain sizes of Ni-Co/ZrO$_2$ coatings prepared in baths with different ZrO$_2$ concentrations, calculated according to the Scherrer equation. The results showed that as the ZrO$_2$ particle concentration was increased, the grain size of the composite coatings first decreased but then increased. The EDX results showed the ZrO$_2$ content to be maximized when the ZrO$_2$ concentration in the bath was 15 g/L. During electrodeposition of a composite coating, particles suspended in the plating solution become adsorbed on the growing metal matrix and inhibit further growth of the crystals while enhancing crystal nucleation. The decrease of grain size may lead to increases in micro-hardness and wear resistance (vide infra).
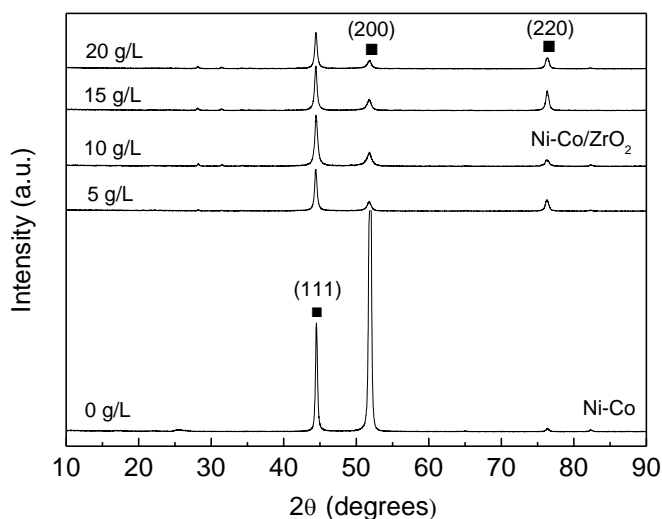
Figure 2. XRD patterns of Ni-Co/ZrO$_2$ coatings prepared in baths containing different ZrO$_2$ concentrations; plating conditions: 45 °C, 1.5 A/dm^2, 30 min.

Table 2. Grain sizes of Ni-Co/ZrO$_2$ coatings prepared in baths with different ZrO$_2$ concentrations, calculated according to the Scherrer equation.

	Ni-Co	Ni-Co/ZrO$_2$ 5 g/L	Ni-Co/ZrO$_2$ 10 g/L	Ni-Co/ZrO$_2$ 15 g/L	Ni-Co/ZrO$_2$ 20 g/L
Grain size (nm) (111)	28.1	22.4	19.7	22.4	22.3
Grain size (nm) (200)	30.4	16.6	16.0	16.3	17.2
Grain size (nm) (220)	31.4	20.9	18.6	23.3	20.2

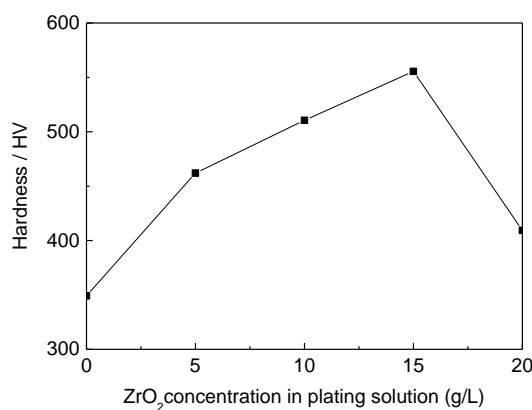*3.3. Micro-hardness of the composite coatings*

Figure 3. Micro-hardnesses of Ni-Co/ZrO$_2$ composite coatings prepared in baths with different ZrO$_2$ concentrations.

Figure 3 shows the micro-hardnesses of the Ni-Co/ZrO$_2$ composite coatings. The micro-hardness increased with increasing ZrO$_2$ concentration. However, when the ZrO$_2$ concentration was increased beyond 15 g/L, the micro-hardness began to decrease. This trend mirrors that in the EDX results. It is worth noting that the highest micro-hardness of the composite coating was 555.54 HV at a bath ZrO$_2$ concentration of 15 g/L, 59% higher than that of the Ni-Co coating. The increased micro-hardness may be attributed to dispersion strengthening and fine-grain strengthening [20]. Pavlatou et al. [20] reported that pure Ni deposits prepared by pulse plating had a finer grain size and showed higher hardness than those prepared by direct current plating. Besides, when SiC was co-deposited with Ni, the hardness of the Ni/SiC deposit was higher than that of a pure Ni deposit, and a deposit prepared by pulse plating showed significantly improved hardness because of grain refinement and higher incorporation of SiC. In our study, as the ZrO$_2$ concentration in the electrolyte was increased, the content of ZrO$_2$ in the composite coatings increased and the grain size decreased. As a result, the micro-hardness increased with increasing ZrO$_2$ concentration. However, when the ZrO$_2$ concentration was excessively high, the agglomeration effect led to a decrease in the micro-hardness.

3.4 Wear resistance of the composite coatings

Weight loss and friction coefficient results are shown in Fig. 4 and Fig. 5. The composite coatings showed better wear resistance than that of the Ni-Co coating. Increased hardness of materials will lead to an increase in wear resistance [21].

In composite co-deposition, ZrO$_2$ particles can accelerate the growth of Ni-Co alloys to form larger stacked Ni-Co/ZrO$_2$ composites. Ni-Co/ZrO$_2$ composite coatings show excellent mechanical properties, such as hardness and anti-wear performance, because of the high hardnesses of both the Ni-Co matrix and ZrO$_2$ particles. Therefore, Ni-Co/ZrO$_2$ coatings show superior anti-wear performance.
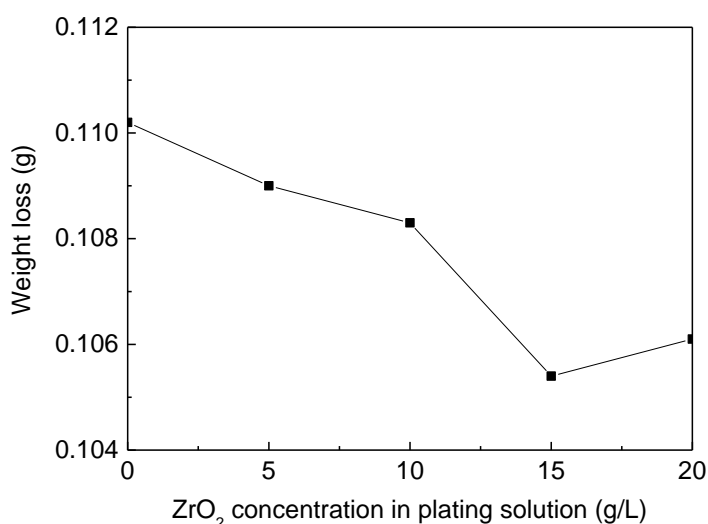

Figure 4. Weight losses of Ni-Co/ZrO$_2$ composite coatings prepared in baths with different ZrO$_2$ concentrations.
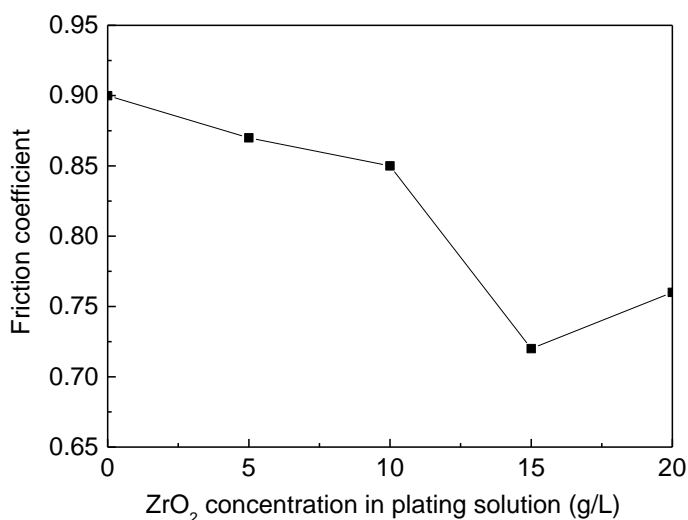
Figure 5. Friction coefficients of Ni-Co/ZrO$_2$ composite coatings prepared in baths with different ZrO$_2$ concentrations.

4. CONCLUSIONS

In this study, Ni-Co/ZrO$_2$ composite coatings have been prepared by electrodeposition from an Ni-Co electrolyte containing suspended ZrO$_2$ particles. The results showed that Ni-Co/ZrO$_2$ composite coatings had higher micro-hardness and anti-wear performance. As the ZrO$_2$ concentration in the bath was increased to 15 g/L, the composite coatings showed the maximum ZrO$_2$ content coupled with the minimum grain size. With increasing ZrO$_2$ content in the coatings, up to the optimum value, the composite coatings show higher micro-hardness and better wear resistance.

References

1. B. Li, W. Zhang, W. Zhang, Y. Huan, *J. Alloys Compd.*, 702 (2017) 38.
2. N. P. Wasekar, S. Madhavi Latha, M. Ramakrishna, D.S. Rao, G. Sundararajan, *Mater. Design*, 112 (2016) 140.
3. M.K. Das, R. Li, J. Qin, X. Zhang, K. Das, A. Thueploy, S. Limpanart, Y. Boonyongmaneerat, M. Ma, R. Liu, *Surf. Coat. Technol.,* 309 (2017) 337.
4. M. Srivastava, V. K. William Grips, K. S. Rajam, *Appl. Surf. Sci.*, 257 (2010) 717.
5. L. Shi, C.F. Sun, F. Zhou, W.M. Liu, *Mater. Sci. Eng. A*, 397 (2005) 190.
6. B. Bakhit, A. Akbari, *J. Alloys Compd.*, 560 (2013) 92.
7. S.W. Jiang, L. Yang, J.N. Pang, H. Lin, Z.Q. Wang, *Surf. Coat. Technol.,* 286 (2016) 197.
8. X. Zhang, J. Qin, T. Perasinjaroen, W. Aeksen, M. K. Das, R. Hao, B. Zhang, P. Wangyao, Y. Boonyongmaneerat, S. Limpanart, M. Ma, R. Liu, *Surf. Coat. Technol.*, 276 (2015) 228.
9. E. Beltowska-Lehman, P. Indyka, A. Bigos, M.J. Szczerba, M. Kot, *Mater. Design*, 80 (2015) 1.
10. E. Beltowska-Lehman, A. Bigos, P. Indyka, A. Chojnacka, A. Drewienkiewicz, S. Zimowski, M. Kot, M.J. Szczerba, *J. Electroanal. Chem.*, 813 (2018) 39.
11. B. Bostani, N. Parvini Ahmadi, S. Yazdani, R. Arghavanian, *Trans. Nonferrous. Met. Soc. China*, 28 (2018) 66.

12. L.P. Wang, Y. Gao, Q.J. Xue, H.W. Liu, T. Xu, *Appl. Surf. Sci.*, 242 (2005) 326.
13. C. Liu, F. Su, J. Liang, *Surf. Coat. Technol.*, 292 (2016) 37.
14. Y.D. Li, H. Jiang, W.H. Huang, H. Tian, *Appl. Surf. Sci.*, 254 (2008) 6865.
15. M. Srivastava, N. Ezhil Selvi, V.K. William Grips, K.S. Rajam, *Surf. Coat. Technol.*, 201 (2006) 3051.
16. M. Zamani, A. Amadeh, S.M. Lari Baghal, *Trans. Nonferrous. Met. Soc. China*, 26 (2016) 484.
17. A. Laszczynska, J. Winiarski, B. Szczygiel, I. Szczygiel, *Appl. Surf. Sci.*, 369 (2016) 224.
18. H. Gul, F. Kilic, M. Uysal, S. Asian, A. Alp, H. Akbulut, *Appl. Surf. Sci.*, 258 (2012) 4260.
19. L. Cheng, L.P. Wang, Z.X. Zeng, T. Xu, *Surf. Coat. Technol.*, 201 (2006) 599.
20. E.A. Pavlatou, M. Stroumbouli, P. Gyftou, N. Spyrellis. *J. Appl. Electrochem.*, 36 (2006) 385.
21. D.H. Jeong, F. Gonzalez, G. Palumbo, K.T. Aust, U. Erb, *Scr. Mater.*, 44 (2001) 493.